Dynamics of the vortex ring loaded with tracer particles in superfluid helium

Robert A. Atherton

Visualising quantum turbulence in superfluid helium makes use of small tracer particles to track the motion of quantized vortices. A key concern when applying this visualisation technique is the effect that the particle itself has on the vortex rings' evolution. In this report, the equations of motion of the vortex ring with a given number of trapped particles are derived and solved using MatLab's built-in function. In particular, the report focuses on the derivation of the tension force and demonstrates that its inclusion causes an increase in the rate of vortex ring radius decay when compared to the evolution without the additional tension force. Finally, a discussion of the implications of this result is presented.

I. Introduction

A lack of flow visualization techniques near absolute zero has stifled the study of quantized vortices[1] in superfluid helium since this research field's inception. Thanks to striking developments, made in the early 2000s, a plethora of reliable visualization techniques have become available. One such technique, known as PIV (particle image velocimeter), involves trapping micron-sized tracer particles, such as solid hydrogen particles, into quantized vortices[2,3]. Subsequent experiments[4,5,6,7] revealed PIV as a favourable technique, with exemplary results being achieved. However, a key factor that needs to be taken into consideration to properly interpret these results, is how the loaded quantized vortices' motion is affected by the presence of the tracer particles themselves. Several theoretical models can be used to understand the interactions between the tracer particles and quantized vortices[8]; the "mutual-interaction" model is explored herein.

The "two-fluid" model of superfluid helium II assumes that at the macroscopic level the superfluid can be modelled as the intimate mixture of two separate fluid types, the superfluid and the normal fluid. The proportion of each fluid type depends on temperature, with the superfluid making up all the fluid at temperatures below around $1K$. The total density ρ of the helium II remains constant in this model and is described by $\rho = \rho_n + \rho_s$ where ρ_n is the density of the normal fluid and ρ_s is the density of the superfluid. The two-fluid model has some limitations but will be the method implemented throughout this report. When focusing specifically on the problem of how particles interact with quantized vortices, a "mutual interaction" model will be used. This model strikes the balance of accuracy and accessibility and hence it is the model focused on during this report. Unlike the "one-way interaction" model, the mutual interaction model considers what effect the particles being trapped in the vortex core has on the evolution of the vortex as opposed to neglecting all influence of the particles. The mutual interaction model was used to generate a series of governing equations of motion which were solved numerically by Barenghi and Sergeev[9] to determine the disturbance to the motion of a quantized ring of radius R by the presence of N tracer particles of radius a. However, whilst deriving the governing equations, a tension force generated by the connection of the ring on the surface of trapped particles was neglected. This tension force is the result of the asymmetry of the vortex line connection on the particle, resulting in a force on the particle in the negative v direction pushing the particle towards the centre of the vortex ring.

The focus of this report will therefore be deriving the tension force $\boldsymbol{F}_T$ and in turn, developing a series of differential equations which will be solved numerically before comparing the solutions to the solutions obtained when no tension force is included. As this force, $\boldsymbol{F}_T$, acts to shrink the radius of the ring, the vortex ring would be expected to decay more quickly when this tension force is included. Then, in turn, the vortex ring would be expected to speed up more quickly. The addition of

this tension force is entirely novel and having a correct working model of how tracer particles affect quantized vortices evolution is key to understanding the results of flow visualisation experiments. Being able to interpret these results allows for advancement in the study of quantum turbulence[10], an area of physics at the cutting edge of physics today. It also allows for the study of vital processes involved with the dynamics of quantum turbulence such as the visualization of individual reconnections of quantized vortices.

II. Method

A quantised ring of radius R with N tracer particles loaded on it is considered. The ring will move through superfluid helium, along the z direction with temperature T. A number, N, tracer particles are trapped in the vortex core, each of which has a mass m and radius a and for simplicity, they are assumed to be neutrally buoyant and remain trapped on the vortex ring throughout the ring's evolution. The forces acting on the vortex ring will be the Magnus force $\boldsymbol{F}_M$ and friction force $\boldsymbol{F}_D$ as well as the Stokes force $\boldsymbol{F}_S$ and additional tension force $\boldsymbol{F}_T$. Working in cylindrical polar coordinates (r, θ, z) the vortex ring's position and velocity will be $\boldsymbol{r}_L = (R, 0, z)$ and $\boldsymbol{V}_L = \left(\dot{R}, 0, \dot{z}\right) = (u, 0, v)$ respectively. The unit vector tangent to the ring in the θ direction will be $\hat{\boldsymbol{\kappa}} = \boldsymbol{\kappa}/\kappa$ and $\boldsymbol{\kappa} = (0, \kappa, 0)$ will be the circulation vector, with $\kappa = 9.97 \times 10^{-4}\ cm^2/s$.

Firstly, the derivation of the additional tension force $\boldsymbol{F}_T$, is presented by focusing on one particle before generalising for multiple particles attached to the vortex ring.

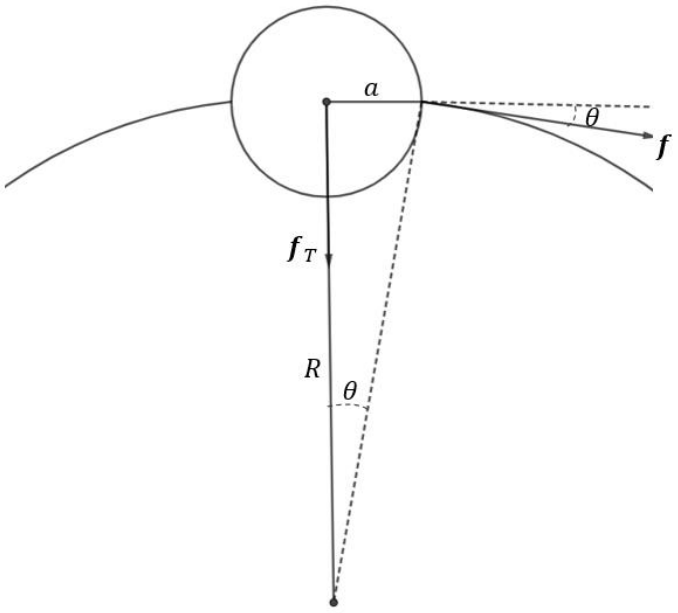

FIG. 1. – Particle with radius a trapped on vortex ring with radius R, acted upon by body force $\boldsymbol{f}$, resultant tension force $\boldsymbol{f}_T$ and angle θ.

Figure 1 shows a simplified model of a single particle trapped in the vortex ring. The force $\boldsymbol{f}$ is a body force which arises due to the connection of the vortex strand to the surface of the particle. As the vortex ring is curved, the connection is asymmetric hence causing the direction of the force to be at an angle we will call θ. The analytic approximation for the force exerted on a particle by a single quantized vortex strand is:

$$\boldsymbol{f} = \frac{\rho_s \kappa^2}{4\pi} \ln\left(\frac{a}{\xi}\right),$$

(1)

as stated by Sergeev and Barenghi[11]. Where $\xi = 10^{-8} cm$ is the vortex core radius or healing length and ρ_s is the superfluid density. By inspection, the two angles in Figure 1 will be the same and $\sin\theta = a/R$. Applying the condition $R \gg a$, and using the small-angle approximation we have $\theta = a/R$. In this case, the resultant force in the horizontal direction will be zero as there is an equally sized force pulling each side of the particle. Therefore, in the vertical direction, the resultant tension force for N particles can be expressed as:

$$\boldsymbol{f}_T = \frac{\rho_s \kappa^2 a}{2\pi R} \ln\left(\frac{a}{\xi}\right) N .$$

(2)

As this force only acts in the negative r direction then:

$$\boldsymbol{F}_T = (-\boldsymbol{f}_T, 0, 0) .$$

(3)

It is assumed that the particle itself does not interact with the vortex ring and the only resultant force is the tension force, meaning the particle remains in a fixed position on the vortex ring. This is, of course, a simplification and there will be a mutual interaction between the trapped particle and the vortex ring. however, this is a fair simplification to make for our means.

The Magnus force, a force generated by a spinning object moving through a fluid, is $\boldsymbol{F}_M = 2\pi R \boldsymbol{f}_M$, where:

$$\boldsymbol{f}_M = \rho_s \boldsymbol{\kappa} \times (\boldsymbol{V}_L - \boldsymbol{V}_{st}) .$$

(4)

$\boldsymbol{V}_{st} = \boldsymbol{V}_s + \boldsymbol{V}_i$ is the total superfluid velocity at the vortex line with $\boldsymbol{V}_i = (0, 0, v_i)$ being the self-induced velocity of the ring, at $T = 0$.

$\boldsymbol{V}_s = (0, 0, v_s)$ is an externally applied superfluid velocity which, for simplicity, is assumed to be only in the z direction and:

$$v_i = \frac{\kappa}{4\pi R}\left[\ln\left(\frac{8R}{\xi}\right) - \frac{1}{2}\right].$$

(5)

The friction force $\boldsymbol{F}_D = 2\pi R \boldsymbol{f}_D$ occurs because of interactions between the vortex core and excitations in the normal fluid, namely phonons and rotons. $\boldsymbol{f}_D$ is expressed as:

$$\boldsymbol{f}_D = \rho_s \kappa [\Gamma_0 (\boldsymbol{V}_n + \boldsymbol{V}_L) + \Gamma_0' \hat{\boldsymbol{\kappa}} \times (\boldsymbol{V}_n - \boldsymbol{V}_L)] ,$$

(6)

with $\boldsymbol{V}_n = (0, 0, v_n)$ which, similarly to $\boldsymbol{V}_s$ is an externally applied velocity in the z direction but in this case, it is the normal fluid velocity rather than the superfluid velocity.

Γ_0 and Γ_0' are dimensionless temperature dependant friction coefficients which were calculated by Barenghi, Donnelly and Vinen[12] to be related to the friction coefficients B and B' via the following two equations:

$$\Gamma_0 = \frac{\rho_n}{2\rho}\frac{B}{[1 - B'\rho_n/(2\rho)]^2 + B^2{\rho_n}^2/(4\rho^2)},$$

(7)

$$\Gamma_0' = \frac{\rho_n}{2\rho}\frac{[B^2\rho_n/(2\rho) - B'(1 - B'\rho_n/(2\rho))]}{[1 - B'\rho_n/(2\rho)]^2 + B^2{\rho_n}^2/(4\rho^2)}.$$

(8)

Where, $\rho = \rho_n + \rho_s$ is the total fluid density.

Finally, there is the Stokes' force which for a vortex ring with total mass mN exerts a force:

$$\boldsymbol{F}_s = 6\pi a\nu_n\rho_n N(\boldsymbol{V}_n - \boldsymbol{V}_L),$$

(9)

where, $\nu_n = \mu/\rho_n$ is the normal fluid kinematic viscosity and μ is the viscosity.

We also have, mass of a particle $m = 4\pi a^3\rho_p/3$ where ρ_p is the particle density. Assuming the tracer particles are neutrally buoyant, this gives $\rho_p = \rho = \rho_n + \rho_s$. This assumption allows for increased simplicity and comparability with some practical experiments[13,14].

Collating these four forces which contribute to the loaded vortex ring's motion, the equations of motion for the vortex ring can be derived:

$$\frac{d\boldsymbol{r}_L}{dt} = \boldsymbol{V}_L,$$

(10)

$$mN\frac{d\boldsymbol{V}_L}{dt} = 2\pi R(\boldsymbol{f}_M + \boldsymbol{f}_D) + \boldsymbol{F}_s + \boldsymbol{F}_T.$$

(11)

Therefore, the resultant equations are:

$$\dot{R} = u,$$

(12)

$$\dot{z} = v,$$

(13)

$$\dot{u} = \frac{2\pi R\rho_s\kappa}{mN}[v - v_s - v_i - \Gamma_0 u + \Gamma_0'(v_n - v)] - \frac{6\pi a\nu_n\rho_n}{m}u - \frac{\rho_s\kappa^2 a}{2\pi R}\ln\left(\frac{a}{\xi}\right)N,$$

(14)

$$\dot{v} = \frac{2\pi R\rho_s\kappa}{mN}[-(1 - \Gamma_0')u + \Gamma_0(v_n - v)] + \frac{6\pi a\nu_n\rho_n}{m}.$$

(15)

Choosing $u = V_o\tilde{u} = (k/R_o)\tilde{u}$, $v = V_o\tilde{v} = (k/R_o)\tilde{v}$, $R = R_o\tilde{R}$, $t = ({R_o}^2/k)\tilde{t}$ and setting $v_n = v_s = 0$ the following system of dimensionless ordinary differential equations (ODEs) are obtained:

$$\dot{\tilde{R}} = \tilde{u}\,,$$

(16)

$$\dot{\tilde{z}} = \tilde{v}\,,$$

(17)

$$\dot{\tilde{u}} = \sigma\tilde{R}[\tilde{v} - \tilde{v_\iota} - \Gamma_0\tilde{u} + \Gamma_0'(\tilde{v_n} - \tilde{v})] - \beta\tilde{u} - \frac{\eta}{\tilde{R}}\,,$$

(18)

$$\dot{\tilde{v}} = \sigma\tilde{R}[-(1 - \Gamma_0')\tilde{u} - \Gamma_0\tilde{v}] - \beta\tilde{v}\,,$$

(19)

where

$$\tilde{v_\iota} = \frac{1}{4\pi\tilde{R}}\left[\gamma + \ln(\tilde{R}) - \frac{1}{2}\right].$$

(20)

With dimensionless constants:

$$\sigma = \frac{2\pi\rho_s {R_o}^3}{mN}\,,\ \gamma = \ln\left(\frac{8R_o}{\xi}\right),\ \beta = \frac{6\pi a\nu_n\rho_n {R_o}^2}{m\kappa}\,,\ \eta = \frac{\rho_s a {R_o}^2}{2\pi m}\ln\left(\frac{a}{\xi}\right).$$

(21)

Using the built in ODE45 function in MatLab and applying the initial conditions:

$$\tilde{R}(0) = 1\,,$$

(22)

$$\tilde{z}(0) = 0\,,$$

(23)

$$\tilde{u}(0) = -\frac{\Gamma_0\tilde{v_\iota}(0)}{(1 - \Gamma_0')^2 + {\Gamma_0}^2}\,,$$

(24)

$$\tilde{v}(0) = \frac{(1 - \Gamma_0')\tilde{v_\iota}(0)}{(1 - \Gamma_0')^2 + {\Gamma_0}^2}\,,$$

(25)

with,

$$\tilde{v_\iota}(0) = \frac{1}{4\pi\tilde{R}}\left[\gamma - \frac{1}{2}\right].$$

(26)

The system of ODEs can be solved with the results obtained outlined and discussed in Section III. Details of the full code used for solving the ODEs can be found in appendix A.

III. Results and Discussion

To relate the results to experiments the parameters chosen were $T = 2K$, $a = 10^{-4}\ cm$ and $R_o = 10^{-2} cm$. To calculate the value of constants (21) data from Donnelly and Barenghi[15] was used. This leads to the following values for the constants to 3 significant figures:

$\beta = 2520, \gamma = 15.9, \eta = 1560$ and; $\sigma = 67000, 33500, 16800, 8380$ as $N = 10, 20, 40, 80$.

Also, from Eqs. (7) and (8) values for Γ_0 and Γ_0' of 0.264 and 0.0626 respectively were obtained. $\tilde{v}_i(0)$ was calculated to be 1.23 to 3.s.f and in turn the initial conditions calculated from Eqs. (24) and (25) were $\tilde{u}(0) = -0.342$ and $\tilde{v}(0) = 1.21$.

Towards the end of the vortex ring's evolution, singularities and other difficulties are experienced as the mathematics begin to break down., hence the cut off points have been chosen to preserve the accuracy of the solutions and allow for appropriate analysis of the vortex ring's evolution. The solutions were generated using MatLab's built-in ODE45 function. The ODE45 function uses the Dormand-Prince method and has an extremely high level of accuracy, delivering values to 16 significant figures. ODE45 uses six function evaluations to calculate fourth and fifth-order solutions, the error is then taken as the difference in these solutions.

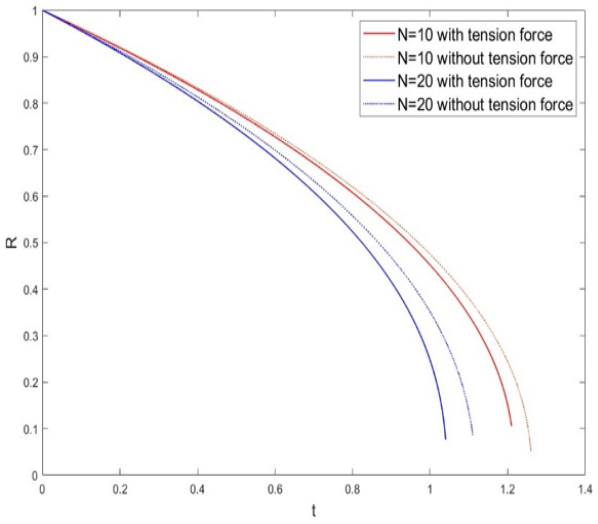

FIG. 2. Dimensionless radius $\tilde{R}$ of the vortex ring vs time $\tilde{t}$ for $N = 10$, $\sigma = 67000$ and $N = 20$, $\sigma = 33500$ with and without the tension force $\boldsymbol{F}_T$.

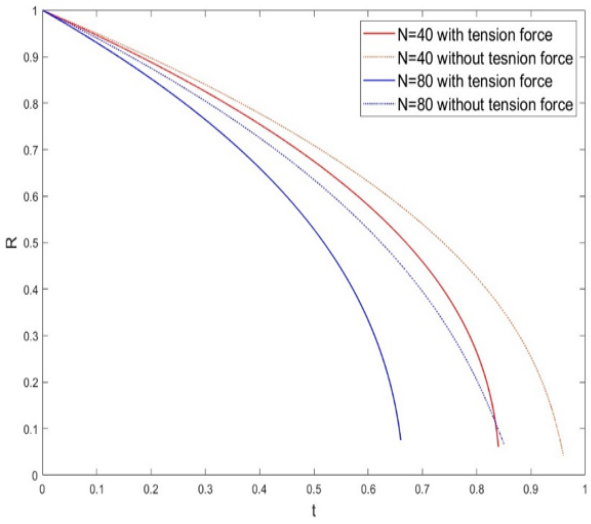

FIG. 3. Dimensionless radius $\tilde{R}$ of the vortex ring vs time $\tilde{t}$ for $N = 40$, $\sigma = 16800$ and $N = 80$, $\sigma = 8380$ with and without the tension force $\boldsymbol{F}_T$.

Figures 2 and 3 show how the radius R of the loaded vortex ring evolves over time t. Figure 2 compares the motion of the ring with and without the additional tension force for number of particles $N = 10, 20$. Figure 3 compares the motion of the ring with and without the additional tension force for number of particles $N = 40, 80$.

Clearly, as the number of particles loaded on the ring increases, (hence σ increasing in turn), the faster the radius of the ring decays. As shown by the time taken to shrink to $0.2\tilde{R}$ reducing from 1.22 to 0.800 when $N = 10$ and $N = 80$ respectively, (both without tension force). Furthermore, it is clear that when comparing the decay of the vortex ring when the tension force is included to when the tension force is not included, the time taken to decay is always lower when the tension force is included. For example, there is a reduction from 1.23 to 1.17 to reach $0.2\tilde{R}$ when $N = 10$. Initially, the difference in ring decay with and without the tension force is negligible however, as the motion evolves this gap becomes more pronounced. This disparity is also much more noticeable as the number of particles N is increased; with the gap between the time taken to reduce to $0.2\tilde{R}$ with and without the tension force, being 0.18 when N=80, as opposed to being just 0.06 when N=10. The result clearly shows that the tension force produces the expected effect of speeding up the vortex ring's decay.

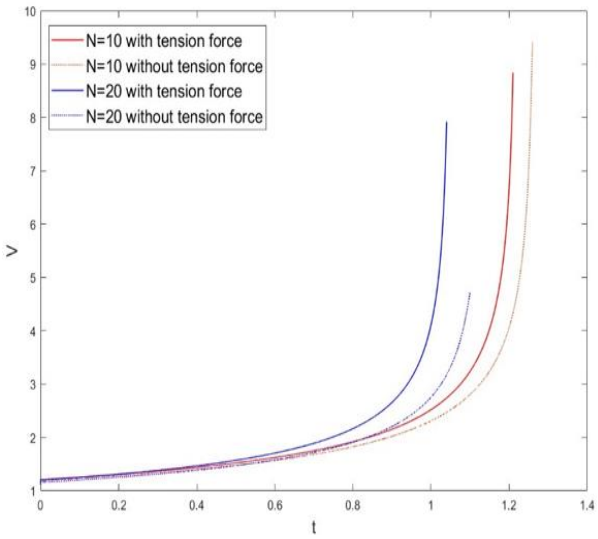

FIG. 4. Dimensionless axial velocity $\tilde{v}$ of the vortex ring vs time $\tilde{t}$ for $N = 10$, $\sigma = 67000$ and $N = 20$, $\sigma = 33500$ with and without the tension force $\boldsymbol{F}_T$.

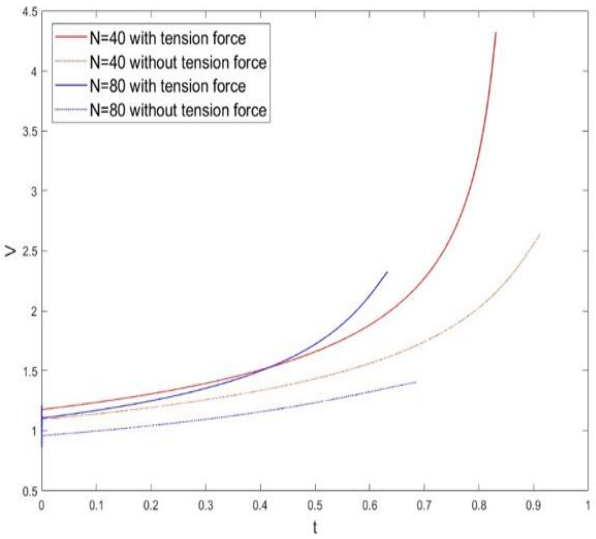

FIG. 5. Dimensionless axial velocity $\tilde{v}$ of the vortex ring vs time $\tilde{t}$ for $N = 40$, $\sigma = 16800$ and $N = 80$, $\sigma = 8380$ with and without the tension force $\boldsymbol{F}_T$.

It follows that as the radius decay is faster when the tension force is included and when N Is increased the axial velocity component $\dot{\tilde{z}} = \tilde{v}$ should also increase. This result is demonstrated in Figures 4 and 5 which show axial velocity against time, with and without the tension force for $N = 10, 20$ in Figure 4 and $N = 40, 80$ in Figure 5. As the radius of the ring shrinks over time the axial velocity increases, as expected, with the time taken to reach $2\tilde{v}$ for $N = 20$ without and with tension force decreasing from 0.830 to 0.750 respectively. As with the radius decay, the effect of the tension force is more prominent when the number of particles is increased with the time taken to reach $2\tilde{v}$ decreasing from 0.775 to 0.575 for the $N = 40$ solution. Figure 4 shows that initially the difference in evolution between the 4 solutions is small however as time advances, the solutions with the additional tension force (solid lines) speed up more quickly. In fact, in Figure 5, the $N = 40$ solution with additional tension force (red solid line) speeds up and overtakes the more heavily loaded $N = 80$ solution (blue dotted line).

Figures 6 and 7 describe how the radial velocity $\dot{\tilde{R}} = \tilde{u}$ evolves over time. Initially, the ring diminishes at a nearly constant rate before decreasing at a faster and faster rate. Also, the rate of radius decrease is higher as N increases and when the tension force is added, when compared with

the same number of tracer particles. The disparity in velocity is once again much more pronounced as the number of particles is increased, with the $N = 40$ solution with tension force (solid red line) decreasing at such a rate that it crosses over and overtakes the $N = 80$ without tension force solution (blue dotted line) at around $t = 0.78$, shown on Figure 7.

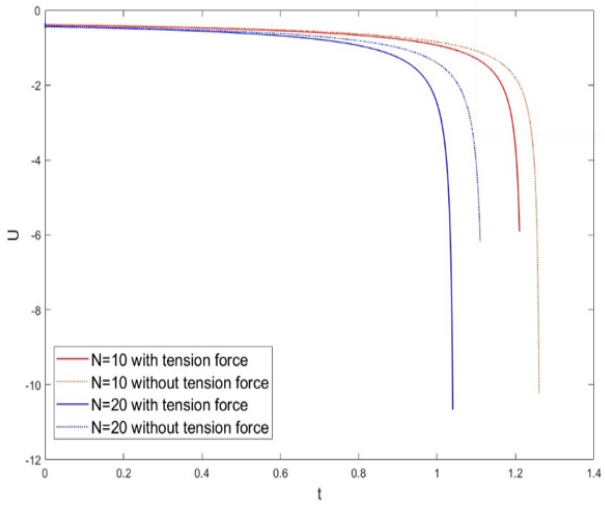

FIG. 6. Dimensionless radial velocity $\tilde{u}$ of the vortex ring vs time $\tilde{t}$ for $N = 10$, $\sigma = 67000$ and $N = 20$, $\sigma = 33500$ with and without the tension force $\boldsymbol{F}_T$.

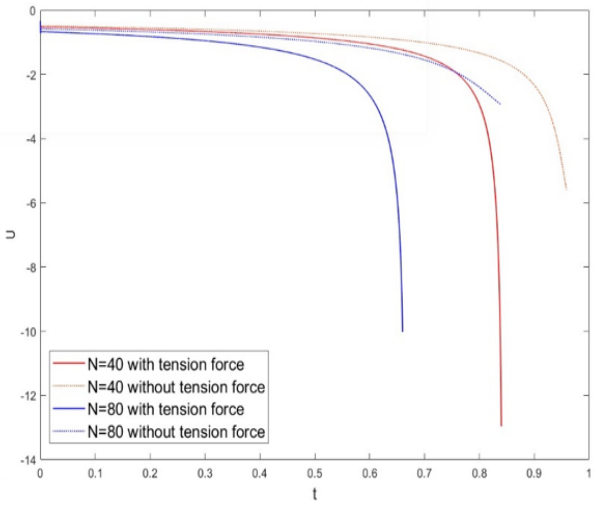

FIG. 7. Dimensionless radial velocity $\tilde{u}$ of the vortex ring vs time $\tilde{t}$ for $N = 40$, $\sigma = 16800$ and $N = 80$, $\sigma = 8380$ with and without the tension force $\boldsymbol{F}_T$.

The results clearly show that, as expected, the additional tension force $\boldsymbol{F}_T$ has increased the rate of vortex ring decay. This provides evidence that the derivation of the force and its implementation into the equations of motion has been implemented successfully, leading to the solutions found being correct and in line with theoretical expectations. Having an accurate, working model of how a particle trapped in the core of a vortex affects its evolution is a crucial tool when analysing and interpreting the results of PIV experiments. In turn, the visualisation of quantum vortices allows for a vast array of research fields to take place, such as the study of velocity statistics, individual quantized vortex reconnections and quantum turbulence itself. Having a deeper understanding of quantum turbulence means having the ability to apply it to long-standing unsolved classical problems; from temporal decay of homogenous, isotropic turbulence to the Loitsianskii invariant. This is since extremely high turbulent flows are needed to tackle these problems and generating these flows in superfluid helium is not a difficult task. However, to visualise, interpret and understand these results is where having an accurate model of how trapped particles affect the motion of the vortex is so valuable.

IV. Conclusion

This report provides clear evidence that the inclusion of the tension force when deriving the equations of motion for a vortex ring loaded with tracer particles, increases the rate of radius decay of the ring throughout its evolution when compared to the case when no tension force is added.

Although having achieved the expected result, as outlined in section III, there are still several interactions which have been overlooked for simplicity which would of course change the model and

its accuracy. To address this and improve the work that has been done here there are several future projects to be undertaken. Firstly, deriving the case for a non-buoyant particle would be a relatively simple adjustment to the model which would make the model more general to accommodate for non-buoyant particles. Furthermore, applying the results seen here to physical experimental data and analysing whether this theoretical model does line up with the data obtained would be of benefit. Finally, defining a quantitative solution to what number of particles can be loaded on a vortex ring before they significantly affect its motion is another potential future project. Having this quantitative solution would allow for the simple application of the results to real-world data, as knowing the number of particles which does not affect the vortices motion allows for more confidence in the results of flow visualization techniques. The knowledge would allow experimenters to know that the motion of the vortex being visualized has not been affected by the loaded tracer particles.

Despite the limitations and future work requirements, the importance of the results presented and their implications for the study of quantum vortices and quantum turbulence should not be overlooked.

[1] R. J. Donnelly, Quantized Vortices in He II Cambridge University Press, Cambridge, (19911)
[2] R. J. Donnelly, A. N. Karpetis, J. J. Niemela, K. R. Sreenivasan, W. F. Vinen, and C. M. White, J. Low Temp. Phys. **126**, 327 (2002); D. Celik and S. W. Van Sciver, Exp. Therm. Fluid Sci. **26**, 971 (2002); T. Zhang, D. Celik, and S. W. Van Sciver, J. Low Temp. Phys. **134**, 985 (2004); T. Zhang and S. W. Van Sciver, ibid. **138**, 865 (2005); Nat. Phys. 1, **36** (2005); G. P. Bewley, D. P. Lathrop, and K. R. Sreenivasan, Nature London **441**, 588 (2006).1
[3] M. S. Paoletti, R. B. Fiorito, K. R. Sreenivasan, and D. P. Lathrop, J. Phys. Soc. Jpn. **77**, 111007 (2008).1
[4] Y. A. Sergeev, S. Wang, E. Meneguz, and C. F. Barenghi, Journal of Low Temperature Physics **146**, 417 (2007).
[5] G. P. Bewley and K. R. Sreenivasan, Journal of Low Temperature Physics 156, 84 (2009).
[6] B. Mastracci and W. Guo, Physical Review Fluids **3**, 063304 (2018)
[7] B. Mastracci, S. Bao, W. Guo, and W. F. Vinen, Physical Review Fluids 4, 083305 (2019)
[8] C. F. Barenghi, Introduction to quantised vortices and turbulence. Chapter 1, in Vortices and Turbulence at Very Low Temperatures, edited by C. F. Barenghi and Y. A. Sergeev, Springer, 2008
[9] C. F. Barenghi and Y. A. Sergeev, Physical Review B **80**, 024514 (2009).
[10] W. Guo, M. La Mantia, D. P. Lathrop, and S. W. Van Sciver, Proceedings of the National Academy of Sciences (USA) **111**, suppl. 1, 4653 (2014).
[11] Y. A. Sergeev and C. F. Barenghi, Particles-Vortex Interactions and Flow Visualization in 4He. Journal of Low Temperature Physics **157**, 429 (2009).
[12] C. F. Barenghi, R. J. Donnelly, and W. F. Vinen, J. Low Temp. Phys. **52**, 189 (1983).4
[13] M. S. Paoletti, M. E. Fisher, K. R. Sreenivasan, and D. P. Lathrop, Phys. Rev. Lett. **101**, 154501 (2008)4.
[14]G. P. Bewley, M. S. Paoletti, K. R. Sreenivasan, and D. P. Lathrop, Proc. Natl. Acad. Sci. U.S.A. **105**, 13707 (20084).
[15] R. J. Donnelly and C. F. Barenghi, The Observed Properties of Liquid Helium at the Saturated Vapor Pressure. Journal of Physical and Chemical Reference Data **27**, 1217 (1998).

Appendix A - *Full Matlab code used for solving system of ODE'*

```
function dydt = N10(t,y)
A = 67000;
C = 0.264;
D = 0.0626;
E = 2520;
dydt = zeros(4,1);
dydt(1) = y(3);
dydt(2) = y(4);
dydt(3) = A*y(1)*(y(4)-(1/(4*pi*y(1)))*(15.9+log(y(1))-1/2)-C*y(3)-D*y(4))-E*y(3);
dydt(4) = A*y(1)*(-(1-D)*y(3)-C*y(4))-E*y(4);
end

function dydt = N10BodyForce(t,y)
A = 67000;
C = 0.264;
D = 0.0626;
E = 2520;
F = 1560;
dydt = zeros(4,1);
dydt(1) = y(3);
dydt(2) = y(4);
dydt(3) = A*y(1)*(y(4)-(1/(4*pi*y(1)))*(15.9+log(y(1))-1/2)-C*y(3)-D*y(4))-E*y(3)-
(F/y(1));
dydt(4) = A*y(1)*(-(1-D)*y(3)-C*y(4))-E*y(4);
end

function dydt = N20(t,y)
A = 33500;
C = 0.264;
D = 0.0626;
E = 2520;
dydt = zeros(4,1);
dydt(1) = y(3);
dydt(2) = y(4);
dydt(3) = A*y(1)*(y(4)-(1/(4*pi*y(1)))*(15.9+log(y(1))-1/2)-C*y(3)-D*y(4))-E*y(3);
dydt(4) = A*y(1)*(-(1-D)*y(3)-C*y(4))-E*y(4);
end

function dydt = N20BodyForce(t,y)
A = 33500;
C = 0.264;
D = 0.0626;
E = 2520;
F = 1560;
dydt = zeros(4,1);
dydt(1) = y(3);
dydt(2) = y(4);
dydt(3) = A*y(1)*(y(4)-(1/(4*pi*y(1)))*(15.9+log(y(1))-1/2)-C*y(3)-D*y(4))-E*y(3)-
(F/y(1));
dydt(4) = A*y(1)*(-(1-D)*y(3)-C*y(4))-E*y(4);
end

function dydt = N40(t,y)
A = 16800;
C = 0.264;
```

```
D = 0.0626;
E = 2520;
dydt = zeros(4,1);
dydt(1) = y(3);
dydt(2) = y(4);
dydt(3) = A*y(1)*(y(4)-(1/(4*pi*y(1)))*(15.9+log(y(1))-1/2)-C*y(3)-D*y(4))-E*y(3);
dydt(4) = A*y(1)*(-(1-D)*y(3)-C*y(4))-E*y(4);
end

function dydt = N40BodyForce(t,y)
A = 16800;
C = 0.264;
D = 0.0626;
E = 2520;
F = 1560;
dydt = zeros(4,1);
dydt(1) = y(3);
dydt(2) = y(4);
dydt(3) = A*y(1)*(y(4)-(1/(4*pi*y(1)))*(15.9+log(y(1))-1/2)-C*y(3)-D*y(4))-E*y(3)-
(F/y(1));
dydt(4) = A*y(1)*(-(1-D)*y(3)-C*y(4))-E*y(4);
end

function dydt = N80(t,y)
A = 8380;
C = 0.264;
D = 0.0626;
E = 2520;
dydt = zeros(4,1);
dydt(1) = y(3);
dydt(2) = y(4);
dydt(3) = A*y(1)*(y(4)-(1/(4*pi*y(1)))*(15.9+log(y(1))-1/2)-C*y(3)-D*y(4))-E*y(3);
dydt(4) = A*y(1)*(-(1-D)*y(3)-C*y(4))-E*y(4);
end

function dydt = N80BodyForce(t,y)
A = 8380;
C = 0.264;
D = 0.0626;
E = 2520;
F = 1560;
dydt = zeros(4,1);
dydt(1) = y(3);
dydt(2) = y(4);
dydt(3) = A*y(1)*(y(4)-(1/(4*pi*y(1)))*(15.9+log(y(1))-1/2)-C*y(3)-D*y(4))-E*y(3)-
(F/y(1));
dydt(4) = A*y(1)*(-(1-D)*y(3)-C*y(4))-E*y(4);
end

%% - Once all functions are saved in the workplace, run the following script to
solve the ODEs and produce the figures. *Figures edited using property editor*

y0 = [1,0,-0.342,1.21];
tspan = [0 1.21];
[t,y] = ode45(@N10BodyForce,tspan,y0);
plot(t,y(:,1),'-')

hold on
```

```
y0 = [1,0,-0.342,1.21];
tspan = [0 1.26];
[t,y] = ode45(@N10,tspan,y0);
plot(t,y(:,1),'-')

hold on

y0 = [1,0,-0.342,1.21];
tspan = [0 1.04];
[t,y] = ode45(@N20BodyForce,tspan,y0);
plot(t,y(:,1),'-')

hold on

y0 = [1,0,-0.342,1.21];
tspan = [0 1.11];
[t,y] = ode45(@N20,tspan,y0);
plot(t,y(:,1),'-')

hold off

y0 = [1,0,-0.342,1.21];
tspan = [0 0.84];
[t,y] = ode45(@N40BodyForce,tspan,y0);
plot(t,y(:,1),'-')

hold on

y0 = [1,0,-0.342,1.21];
tspan = [0 0.96];
[t,y] = ode45(@N40,tspan,y0);
plot(t,y(:,1),'-')

hold on

y0 = [1,0,-0.342,1.21];
tspan = [0 0.66];
[t,y] = ode45(@N80BodyForce,tspan,y0);
plot(t,y(:,1),'-')

hold on

y0 = [1,0,-0.342,1.21];
tspan = [0 0.85];
[t,y] = ode45(@N80,tspan,y0);
plot(t,y(:,1),'-')

hold off

y0 = [1,0,-0.342,1.21];
tspan = [0 1.21];
[t,y] = ode45(@N10BodyForce,tspan,y0);
plot(t,y(:,3),':')

hold on

y0 = [1,0,-0.342,1.21];
tspan = [0 1.26];
[t,y] = ode45(@N10,tspan,y0);
```

```
plot(t,y(:,3),'-')

hold on

y0 = [1,0,-0.342,1.21];
tspan = [0 1.04];
[t,y] = ode45(@N20BodyForce,tspan,y0);
plot(t,y(:,3),'-')

hold on

y0 = [1,0,-0.342,1.21];
tspan = [0 1.11];
[t,y] = ode45(@N20,tspan,y0);
plot(t,y(:,3),'-')

hold off

y0 = [1,0,-0.342,1.21];
tspan = [0 0.840];
[t,y] = ode45(@N40BodyForce,tspan,y0);
plot(t,y(:,3),'-')

hold on

y0 = [1,0,-0.342,1.21];
tspan = [0 0.959];
[t,y] = ode45(@N40,tspan,y0);
plot(t,y(:,3),'-')

hold on

y0 = [1,0,-0.342,1.21];
tspan = [0 0.660];
[t,y] = ode45(@N80BodyForce,tspan,y0);
plot(t,y(:,3),'-')

hold on

y0 = [1,0,-0.342,1.21];
tspan = [0 0.839];
[t,y] = ode45(@N80,tspan,y0);
plot(t,y(:,3),'-')

hold off

y0 = [1,0,-0.342,1.21];
tspan = [0 1.21];
[t,y] = ode45(@N10BodyForce,tspan,y0);
plot(t,y(:,4),'-')

hold on

y0 = [1,0,-0.342,1.21];
tspan = [0 1.26];
[t,y] = ode45(@N10,tspan,y0);
plot(t,y(:,4),'-')
```

```
hold on

y0 = [1,0,-0.342,1.21];
tspan = [0 1.04];
[t,y] = ode45(@N20BodyForce,tspan,y0);
plot(t,y(:,4),'-')

hold on

y0 = [1,0,-0.342,1.21];
tspan = [0 1.10];
[t,y] = ode45(@N20,tspan,y0);
plot(t,y(:,4),'-')

hold off

y0 = [1,0,-0.342,1.21];
tspan = [0 0.831];
[t,y] = ode45(@N40BodyForce,tspan,y0);
plot(t,y(:,4),'-')

hold on

y0 = [1,0,-0.342,1.21];
tspan = [0 0.912];
[t,y] = ode45(@N40,tspan,y0);
plot(t,y(:,4),'-')


hold on

y0 = [1,0,-0.342,1.21];
tspan = [0 0.633];
[t,y] = ode45(@N80BodyForce,tspan,y0);
plot(t,y(:,4),'-')

hold on

y0 = [1,0,-0.342,1.21];
tspan = [0 0.686];
[t,y] = ode45(@N80,tspan,y0);
plot(t,y(:,4),'-')

hold off
```